Available online at www.sciencedirect.com
SCIENCE DIRECT®
ELSEVIER
International Journal of Solids and Structures 42 (2005) 6003–6014
INTERNATIONAL JOURNAL OF SOLIDS and STRUCTURES
www.elsevier.com/locate/ijsolstr

A frequency-domain FEM approach based on implicit Green's functions for non-linear dynamic analysis

D. Soares Jr., W.J. Mansur *

Department of Civil Engineering, COPPE/Federal University of Rio de Janeiro, CP 68506, CEP 21945-970, Rio de Janeiro, RJ, Brazil

Received 17 February 2004; received in revised form 25 May 2005
Available online 20 July 2005

Abstract

The present paper describes an efficient algorithm to integrate the equations of motion implicitly in the frequency domain. The standard FEM displacement model (Galerkin formulation) is employed to perform space discretization, and the time-marching process is carried out through an algorithm based on the Green's function of the mechanical system in nodal coordinates. In the present formulation, mechanical system Green's functions are implicitly calculated in the frequency domain. Once the Green's functions related matrices are computed, a time integration procedure, which demands low computational effort when applied to non-linear mechanical systems, becomes available. At the end of the paper numerical examples are presented in order to illustrate the accuracy of the present approach.
© 2005 Elsevier Ltd. All rights reserved.

Keywords: Green's function; Nodal coordinates; Frequency domain; FEM; Dynamics; Non-linear calculations

1. Introduction

The engineer engaged in dynamic analysis of structures usually employs both time domain and/or transformed domain approaches (Laplace, Fourier, Wavelets, etc.).

Standard frequency-domain approaches based on DFT/FFT algorithms (Bracewell, 1986; Oppenheim and Schafer, 1989; Proakis and Manolakis, 1996) have proved to be a very powerful tool in the design of structural systems (Veletsos and Ventura, 1984; Veletsos and Ventura, 1985; Clough and Penzien,

* Corresponding author. Tel.: +55 21 280 993; fax: +55 21 280 9545.
E-mail address: webe@coc.ufrj.br (W.J. Mansur).

0020-7683/$ - see front matter © 2005 Elsevier Ltd. All rights reserved.
doi:10.1016/j.ijsolstr.2005.05.047

1993; Newland, 1993; Paz, 1997; Mansur et al., 2004). Numerical approaches for soil–structure interaction (SSI) modeling have been the subject of intensive research over the last forty years. In a great deal of the published research work, the soil is modeled by equivalent mass-spring–dashpot systems with frequency dependent properties; i.e., a frequency-domain strategy is adopted (Liu and Fagel, 1971; Jennings and Bielak, 1973; Wolf, 1985; Wu and Smith, 1995). Frequency-domain approaches are also most suitable in many other cases, e.g., (a) when damping properties are frequency dependent, dynamic modeling of structures being a typical case (Theodorsen and Garrick, 1940; Myklestad, 1952; Bishop, 1955; Newmark, 1957; Crandall, 1963, 1970, 1991; Makris, 1997; Makris and Zhang, 2000); (b) when the knowledge of the frequency spectrum is necessary (Takewaki and Nakamura, 2000); etc.

In recent years a number of time/frequency-domain strategies (hybrid, implicit, etc.) have been developed, making it possible to carry out non-linear analyses of mechanical systems having frequency dependent properties (Matthees, 1982; Kawamoto, 1983; Wolf, 1985; Venâncio-Filho and Claret, 1991, 1992; Aprile et al., 1994; Mansur et al., 2000; Soares Jr. and Mansur, 2003).

Venancio-Filho and Claret (1992) and later on Mansur et al. (2000) presented an Implicit Fourier Transform algorithm (ImFT), where modal coordinates are used to uncouple the equations of motion and the pseudo-force method is used to deal with non-linear effects and non-proportional damping. Later on Soares Jr. and Mansur (2003) showed that the first column of the ImFT algorithm matrix corresponding to a particular mode is the time domain discrete Green's function of the SDOF equilibrium equation of that mode computed by applying a discrete inverse Fourier transform algorithm (IFFT) to the corresponding frequency-domain transfer function. Thus it became clear that the ImFT approach is in fact a standard convolution procedure (see Mansur, 1983; Dominguez, 1993) being the time domain Green's function capable of implicitly account for frequency dependent properties. Soares Jr. and Mansur (2003) presented the UFTD (unified frequency/time domain) algorithm, which is a modal step-by-step explicit frequency/time domain procedure that can consider frequency dependent properties; the authors report the UFTD approach as a stable and efficient explicit step-by-step algorithm.

Nowadays, one can find papers based on the mechanical system Green's function employing the FEM in nodal coordinates only in time domain (Fung, 1997; Soares Jr. and Mansur, 2005). The present work reports a unified step-by-step time/frequency-domain algorithm to integrate the FEM (Hughes, 1987; Zienkiewicz and Taylor, 1989; Bathe, 1996) equations of motion in nodal coordinates. The time domain Green's function is computed from the corresponding mechanical system frequency-domain transfer function by a modified DFT procedure. The approach presented here gives accurate and stable results, as illustrated by two examples (one linear and one non-linear), presented at the end of the paper.

Moreover, the formulation here reported can also be employed to deal with initial conditions, as an alternative approach to that previously reported by Mansur et al. (2004). Mansur et al. (2004) presented a procedure that can consider contributions due to non-null initial conditions when standard DFT/FFT frequency-domain algorithms are employed. The present paper, on the other hand, presents a step-by-step hybrid time/frequency-domain procedure. It is also important to observe that, as mentioned above, the present work differs substantially from that by Soares Jr. and Mansur (2003) as the former paper's formulation employs nodal coordinates whereas the later employs modal coordinates.

2. Model equations

The finite element method equilibrium equation, which governs the linear response of a dynamic system, is given by (Hughes, 1987; Zienkiewicz and Taylor, 1989; Clough and Penzien, 1993; Bathe, 1996; Paz, 1997)

$$\mathbf{M}\ddot{\mathbf{U}}(t) + \mathbf{C}\dot{\mathbf{U}}(t) + \mathbf{K}\mathbf{U}(t) = \mathbf{R}(t) \tag{1}$$

where **M**, **C** and **K** are mass, damping and stiffness matrices respectively; $\mathbf{R}(t)$ is the nodal equivalent force vector; $\mathbf{U}(t)$, $\dot{\mathbf{U}}(t)$ and $\ddot{\mathbf{U}}(t)$ are respectively displacement, velocity and acceleration nodal vectors originated from the finite element method spatial discretization.

The analytical expressions for the displacement $\mathbf{U}(t)$ and the velocity $\dot{\mathbf{U}}(t)$ vectors, which obey Eq. (1), are given by

$$\begin{aligned}\mathbf{U}(t) &= \mathbf{G}(t)\mathbf{C}\mathbf{U}(0) + \dot{\mathbf{G}}(t)\mathbf{M}\mathbf{U}(0) + \mathbf{G}(t)\mathbf{M}\dot{\mathbf{U}}(0) + \mathbf{G}(t) \bullet \mathbf{R}(t)\\ \dot{\mathbf{U}}(t) &= -\mathbf{G}(t)\mathbf{K}\mathbf{U}(0) + \dot{\mathbf{G}}(t)\mathbf{M}\dot{\mathbf{U}}(0) + \dot{\mathbf{G}}(t) \bullet \mathbf{R}(t)\end{aligned} \tag{2}$$

where $\mathbf{U}(0)$ and $\dot{\mathbf{U}}(0)$ stand for initial displacement and initial velocity, respectively; $\mathbf{G}(t)$ represents the Green's function matrix of the model; and the symbol $\bullet$ represents convolution. The j column of $\mathbf{G}(t)$, $\mathbf{g}_j(t)$, can be obtained through the solution of Eq. (1) for an impulsive load applied at node j, i.e., for a nodal equivalent force vector given by

$$\mathbf{R}(t) = \mathbf{1}_j \delta(t-0) \tag{3}$$

where $\delta(t-0)$ is the Dirac delta function and $\mathbf{1}_j$ is a unit base vector, i.e., $1_{ij} = \delta_{ij}$, δ_{ij} being the Kroenecker delta.

In the present discussion, $\mathbf{g}_j(t)$ can be computed more conveniently by considering an initial velocity vector such that the identity *impulse = momentum variation* is verified, i.e.,

$$\mathbf{M}\dot{\mathbf{g}}_j(0) = \mathbf{1}_j \int_{-\infty}^{+\infty} \delta(t-0)\,\mathrm{d}t \tag{4}$$

Thus

$$\dot{\mathbf{g}}_j(0) = \mathbf{M}^{-1}\mathbf{1}_j \tag{5}$$

Therefore

$$\dot{\mathbf{G}}(0) = \mathbf{M}^{-1}\mathbf{I} = \mathbf{M}^{-1} \quad \text{and} \quad \mathbf{G}(0) = \mathbf{0} \tag{6}$$

The method considered here for the numerical solution of Eq. (2) does not use any analytical expression for the problem Green's function; rather it employs an implicit frequency-domain procedure to compute numerically the Green's function matrix and its time derivative. The convolution integrals indicated in expression (2) are conveniently approximated as specified in Eq. (8).

Eq. (2) at time Δt reads

$$\begin{aligned}\mathbf{U}(\Delta t) &= \mathbf{G}(\Delta t)\mathbf{C}\mathbf{U}(0) + \dot{\mathbf{G}}(\Delta t)\mathbf{M}\mathbf{U}(0) + \mathbf{G}(\Delta t)\mathbf{M}\dot{\mathbf{U}}(0) + \int_0^{\Delta t} \mathbf{G}(\Delta t - \tau)\mathbf{R}(\tau)\,\mathrm{d}\tau\\ \dot{\mathbf{U}}(\Delta t) &= -\mathbf{G}(\Delta t)\mathbf{K}\mathbf{U}(0) + \dot{\mathbf{G}}(\Delta t)\mathbf{M}\dot{\mathbf{U}}(0) + \int_0^{\Delta t} \dot{\mathbf{G}}(\Delta t - \tau)\mathbf{R}(\tau)\,\mathrm{d}\tau\end{aligned} \tag{7}$$

Assuming that Δt is small enough, the following approximations can replace the integrals indicated in Eq. (7):

$$\begin{aligned}\int_0^{\Delta t} \mathbf{G}(\Delta t - \tau)\mathbf{R}(\tau)\,\mathrm{d}\tau &\approx \mathbf{G}(0)\mathbf{R}(\Delta t)\Delta t\\ \int_0^{\Delta t} \dot{\mathbf{G}}(\Delta t - \tau)\mathbf{R}(\tau)\,\mathrm{d}\tau &\approx \dot{\mathbf{G}}(0)\mathbf{R}(\Delta t)\Delta t\end{aligned} \tag{8}$$

Considering Eq. (7), as well as the approximations indicated by Eq. (8), recursive expressions can be obtained by considering Eq. (2) at the time $t + \Delta t$ and by supposing that the analysis starts at the time t. The recurrence relations, that arise, are given by

$$\begin{aligned}\mathbf{U}(t+\Delta t) &= \lfloor \mathbf{G}(\Delta t)\mathbf{C} + \dot{\mathbf{G}}(\Delta t)\mathbf{M} \rfloor \mathbf{U}(t) + \mathbf{G}(\Delta t)\mathbf{M}\dot{\mathbf{U}}(t) + \mathbf{G}(0)\mathbf{R}(t+\Delta t)\Delta t \\ \dot{\mathbf{U}}(t+\Delta t) &= -\mathbf{G}(\Delta t)\mathbf{K}\mathbf{U}(t) + \dot{\mathbf{G}}(\Delta t)\mathbf{M}\dot{\mathbf{U}}(t) + \dot{\mathbf{G}}(0)\mathbf{R}(t+\Delta t)\Delta t\end{aligned} \tag{9}$$

where $\mathbf{G}(\Delta t)$ represents the solution of Eq. (1), at the time instant Δt, considering the load cases corresponding to prescribed initial velocity vectors given by the columns of $\mathbf{M}^{-1}$ (Eq. (6)). It must be observed that $\mathbf{G}(0) = \mathbf{0}$; thus the last term on the r.h.s. of the first equation of expression (9) is null.

3. Implicit frequency-domain analysis

In order to develop the ImFGA (Implicit Frequency-domain Green's Approach), one should obtain the matrices $\mathbf{G}(\Delta t)$ and $\dot{\mathbf{G}}(\Delta t)$ (see Eq. (9)) implicitly in the frequency domain. Thus the time domain Green's function matrices must be expressed in terms of harmonic components.

The transient Green's function and its derivative ($\mathbf{G}(t)$ and $\dot{\mathbf{G}}(t)$) may be related to their steady-state counterpart ($\overline{\mathbf{G}}_v(t)$ and $\dot{\overline{\mathbf{G}}}_v(t)$, respectively) by the equations

$$\begin{aligned}\mathbf{G}(t) &= \overline{\mathbf{G}}_v(t) + \overline{\mathbf{G}}(t) \\ \dot{\mathbf{G}}(t) &= \dot{\overline{\mathbf{G}}}_v(t) + \dot{\overline{\mathbf{G}}}(t)\end{aligned} \tag{10}$$

in which $\overline{\mathbf{G}}(t)$, as well as $\dot{\overline{\mathbf{G}}}(t)$, are corrective functions representing the effect of unsatisfied initial conditions. The corrective displacement and velocity functions may be expressed as

$$\begin{aligned}\overline{\mathbf{G}}(t) &= c_u\overline{\mathbf{G}}_u(t) + c_v\overline{\mathbf{G}}_v(t) \\ \dot{\overline{\mathbf{G}}}(t) &= c_u\dot{\overline{\mathbf{G}}}_u(t) + c_v\dot{\overline{\mathbf{G}}}_v(t)\end{aligned} \tag{11}$$

where $\overline{\mathbf{G}}_u(t)$ is the steady-state displacement at a time $0 < t < t_o$ due to a periodic set of unit displacement changes applied at intervals t_o and $\overline{\mathbf{G}}_v(t)$ is the corresponding displacement due to a periodic set of unit velocity changes applied at the same intervals.

The constants c_u and c_v present in Eq. (11) can be computed from the conditions $\mathbf{G}(0) = \overline{\mathbf{G}}_v(0) + \overline{\mathbf{G}}(0)$ and $\dot{\mathbf{G}}(0) = \dot{\overline{\mathbf{G}}}_v(0) + \dot{\overline{\mathbf{G}}}(0)$. Taking into account c_u and c_v computed as described, and Eqs. (11) and (6), Eq. (10) becomes

$$\begin{aligned}\mathbf{G}(t) &= \mathbf{\Theta}\left[\overline{\mathbf{G}}_v(t) - \overline{\mathbf{G}}_v(0)\overline{\mathbf{G}}_u^{-1}(0)\overline{\mathbf{G}}_u(t)\right] \\ \dot{\mathbf{G}}(t) &= \mathbf{\Theta}\left[\dot{\overline{\mathbf{G}}}_v(t) - \overline{\mathbf{G}}_v(0)\overline{\mathbf{G}}_u^{-1}(0)\dot{\overline{\mathbf{G}}}_u(t)\right]\end{aligned} \tag{12}$$

where

$$\mathbf{\Theta} = \mathbf{M}^{-1}\left[\overline{\mathbf{G}}_v(0) - \overline{\mathbf{G}}_v(0)\overline{\mathbf{G}}_u^{-1}(0)\dot{\overline{\mathbf{G}}}_u(0)\right]^{-1} \tag{13}$$

Using Eq. (12) one can obtain $\mathbf{G}(\Delta t)$ and $\dot{\mathbf{G}}(\Delta t)$, once the values for $\overline{\mathbf{G}}_u(0)$, $\dot{\overline{\mathbf{G}}}_u(0)$, $\overline{\mathbf{G}}_v(0)$, $\dot{\overline{\mathbf{G}}}_v(0)$, $\overline{\mathbf{G}}_u(\Delta t)$, $\dot{\overline{\mathbf{G}}}_u(\Delta t)$, $\overline{\mathbf{G}}_v(\Delta t)$ and $\dot{\overline{\mathbf{G}}}_v(\Delta t)$ are known. The expressions for the above-required matrices can be obtained by a generalization of the concepts presented previously (Veletsos and Ventura, 1984; Veletsos and Ventura, 1985; Soares Jr. and Mansur, 2003) for the single-degree-of-freedom (SDOF) case, as indicated next

$$\overline{\mathbf{G}}_v(0) = \mathbf{M}\boldsymbol{\Omega} + \alpha\mathbf{I} \tag{14}$$

$$\overline{\mathbf{G}}_u(0) = (1/2)\mathbf{I} + (1/\Delta t)\mathbf{C}\mathbf{K}^{-1} - \mathbf{K}\,\widehat{\boldsymbol{\Omega}} \tag{15}$$

$$\dot{\overline{\mathbf{G}}}_v(0) = \overline{\mathbf{G}}_u(0) - \mathbf{C}\boldsymbol{\Omega} - \alpha\mathbf{C}\mathbf{M}^{-1} \tag{16}$$

$$\dot{\overline{\mathbf{G}}}_u(0) = -\mathbf{K}\boldsymbol{\Omega} - \alpha\mathbf{K}\mathbf{M}^{-1} \tag{17}$$

$$\overline{\mathbf{G}}_v(\Delta t) = \overline{\mathbf{G}}_v(0) \tag{18}$$

$$\overline{\mathbf{G}}_u(\Delta t) = \overline{\mathbf{G}}_u(0) - \mathbf{I} \tag{19}$$

$$\dot{\overline{\mathbf{G}}}_v(\Delta t) = \dot{\overline{\mathbf{G}}}_v(0) - \mathbf{I} \tag{20}$$

$$\dot{\overline{\mathbf{G}}}_u(\Delta t) = \dot{\overline{\mathbf{G}}}_u(0) \tag{21}$$

where

$$\alpha = \frac{\Delta t}{2}\left(\frac{1}{\pi^2}\sum_{m=1}^{MT}\left\{\frac{1}{m^2}\right\} - \frac{1}{6}\right) \tag{22}$$

$$\boldsymbol{\Omega} = \frac{1}{\Delta t}\sum_{m=-MT}^{MT}\left\{\left[-\left(\frac{2\pi m}{\Delta t}\right)^2\mathbf{M} + \left(\frac{2\pi m}{\Delta t}i\right)\mathbf{C} + \mathbf{K}\right]^{-1}\right\} \tag{23}$$

$$\widehat{\boldsymbol{\Omega}} = \frac{1}{\Delta t}\sum_{\substack{m=-MT \\ m\neq 0}}^{MT}\left\{\left[-\left(\frac{2\pi m}{\Delta t}\right)^2\mathbf{M} + \left(\frac{2\pi m}{\Delta t}i\right)\mathbf{C} + \mathbf{K}\right]^{-1} \Big/ \left(\frac{2\pi m}{\Delta t}i\right)\right\} \tag{24}$$

and $\mathbf{I}$ is the identity matrix.

Once $\mathbf{G}(\Delta t)$ and $\dot{\mathbf{G}}(\Delta t)$ have been calculated (see expressions (12)–(24)), one can use Eq. (9) to compute unknown displacements and velocities for each time-step of the analysis. Eq. (9) can be written in a more compact way, as follows:

$$\begin{aligned}\mathbf{U}(t+\Delta t) &= \boldsymbol{\Phi}_1\mathbf{U}(t) + \boldsymbol{\Phi}_2\dot{\mathbf{U}}(t)\\ \dot{\mathbf{U}}(t+\Delta t) &= \dot{\boldsymbol{\Phi}}_1\mathbf{U}(t) + \dot{\boldsymbol{\Phi}}_2\dot{\mathbf{U}}(t) + \mathbf{M}^{-1}\mathbf{R}(t+\Delta t)\Delta t\end{aligned} \tag{25}$$

where Eq. (6) were taken into account and

$$\begin{aligned}\boldsymbol{\Phi}_1 &= \mathbf{G}(\Delta t)\mathbf{C} + \dot{\mathbf{G}}(\Delta t)\mathbf{M}\\ \boldsymbol{\Phi}_2 &= \mathbf{G}(\Delta t)\mathbf{M}\\ \dot{\boldsymbol{\Phi}}_1 &= -\mathbf{G}(\Delta t)\mathbf{K}\\ \dot{\boldsymbol{\Phi}}_2 &= \dot{\mathbf{G}}(\Delta t)\mathbf{M}\end{aligned} \tag{26}$$

The final recursive relations (Eq. (25)) lead to an efficient step-by-step procedure, once lumped mass matrix is considered.

In order to correctly evaluate matrices $\mathbf{G}(\Delta t)$ and $\dot{\mathbf{G}}(\Delta t)$, and as a consequence the whole solution algorithm, a good choice of MT (see Eqs. (22)–(24)) is required. It can be observed that for $MT = 1$, good results are in most cases achieved (it depends on the physical properties of the mechanical system, as well as of the time-step discretization considered). Fig. 1 shows the spectral radius of the amplification matrix, for the SDOF problem (Hughes, 1987; Bathe, 1996), versus time-step. Different natural frequencies, damping ratios and methodologies have been considered. As it can be seen in Fig. 1, it is possible to obtain

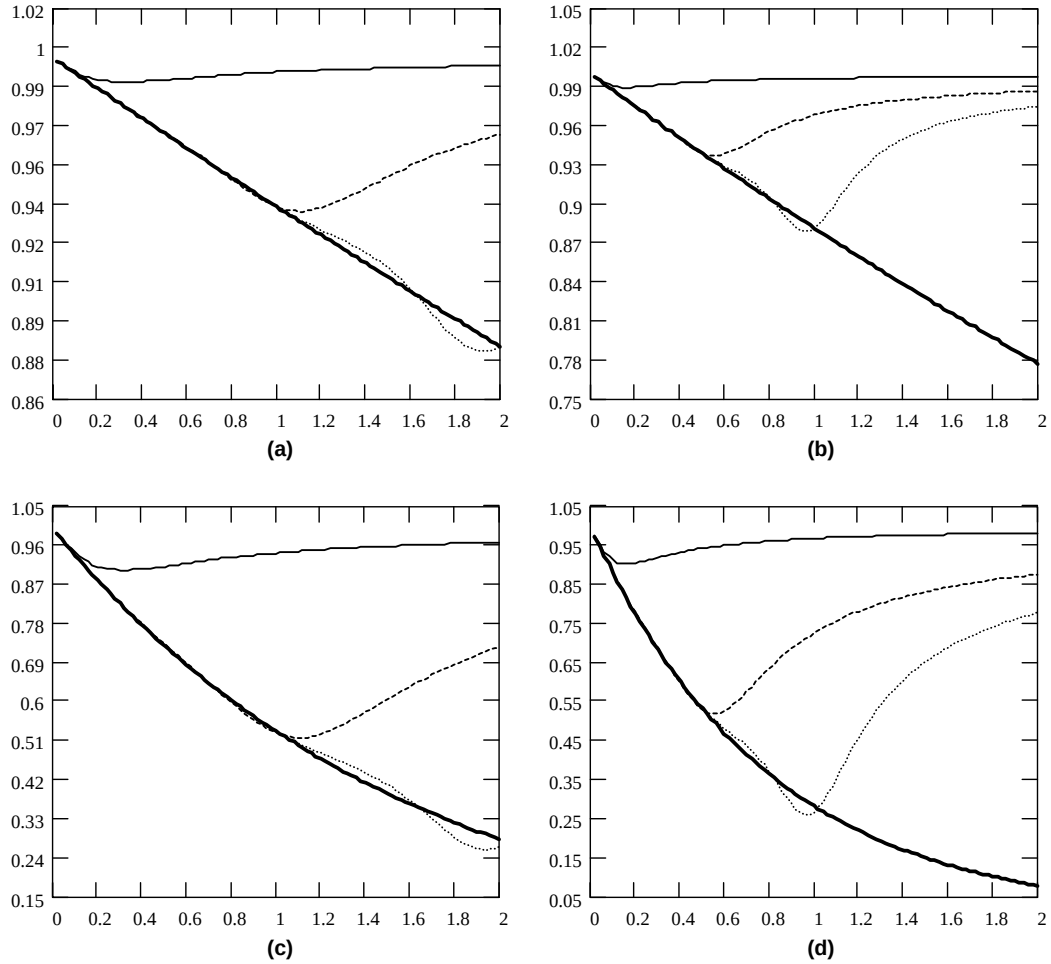

Fig. 1. Spectral radius of the SDOF amplification matrix versus time-step ($\rho \times \Delta t$) considering different natural frequencies and damping ratios: (a) $w = 2\pi$, $\delta = 1\%$; (b) $w = 4\pi$, $\delta = 1\%$; (c) $w = 2\pi$, $\delta = 10\%$; (d) $w = 4\pi$, $\delta = 10\%$. Methodologies employed: analytical (—); (—) trapezoidal rule; (– – –) ImFGA with $MT = 1$; (···) ImFGA with $MT = 2$.

an amplification matrix whose spectral radius is closer to that of the analytical one, by the use of the present implicit frequency-domain formulation (even with small values of MT) than by the use of the classical Newmark trapezoidal rule method.

The simplifications adopted in Eq. (8) are responsible for the major contribution of the present formulation to response errors. These simplifications, however, are typical of frequency-domain analyses: classical procedures, e.g., those based on DFT/FFT algorithms, also adopt exactly them, however, as the equations are written in a different manner, such simplifications are not as clearly displayed as here (Bracewell, 1986; Oppenheim and Schafer, 1989; Soares Jr. and Mansur, 2003). The simplifications indicated by Eq. (8) reduce substantially the cost of the non-linear analysis algorithm, which is considered in the next section.

The fact that good precision is achieved with very small MT values makes the present formulation more efficient than standard ones, when frequency-domain analyses employing nodal coordinates are considered. The present formulation is especially efficient for non-linear models.

4. Non-linear analysis

The dynamic finite element method equations for physically non-linear problems can be written as

$$\mathbf{M}\ddot{\mathbf{U}}(t) + \mathbf{C}\dot{\mathbf{U}}(t) + \mathbf{F}(\mathbf{U}(t)) = \mathbf{R}(t) \tag{27}$$

where $\mathbf{F}$ is a vector of elastic or elasto-plastic forces which depends of the nodal unknown displacement vector $\mathbf{U}(t)$. $\mathbf{F}(\mathbf{U}(t))$ represents the vector of nodal forces equivalent to the actual stress state.

In order to deal with the model non-linearity, the pseudo-forces method is adopted here. Such a procedure is adequate for non-linear problems with small strains; as for instance is the case of elasto-plastic behavior of certain structural systems.

Considering the non-linear contributions as pseudo-forces, Eq. (1) can be written as (Soares Jr. and Mansur, 2005)

$$\mathbf{M}\ddot{\mathbf{U}}(t) + \mathbf{C}\dot{\mathbf{U}}(t) + \mathbf{K}_{\mathrm{L}}\mathbf{U}(t) = \mathbf{R}(t) + \mathbf{S}(t) \tag{28}$$

where

$$\mathbf{S}(t) = -\mathbf{K}_{\mathrm{NL}}(\mathbf{U}(t))\mathbf{U}(t) \tag{29}$$

is the pseudo-forces vector; $\mathbf{K}_{\mathrm{L}}$ is the linear stiffness matrix; and $\mathbf{K}_{\mathrm{NL}}$ is the matrix responsible for non-linear contributions, whose elements depend on the displacement vector $\mathbf{U}(t)$.

The solution algorithm represented by Eq. (25) can then, by use of pseudo-forces, easily be adapted to consider non-linear problems, as it is shown below

$$\begin{aligned} \mathbf{U}(t+\Delta t) &= \mathbf{\Phi}_1\mathbf{U}(t) + \mathbf{\Phi}_2\dot{\mathbf{U}}(t) \\ \dot{\mathbf{U}}(t+\Delta t) &= \dot{\mathbf{\Phi}}_1\mathbf{U}(t) + \dot{\mathbf{\Phi}}_2\dot{\mathbf{U}}(t) + \mathbf{M}^{-1}[\mathbf{R}(t+\Delta t) + \mathbf{S}(t+\Delta t)]\Delta t \end{aligned} \tag{30}$$

Eq. (30) show that the ImFGA requires no iterative process. Iterations usually associated to non-linear analyses become unnecessary here as in the ImFGA the computation of the displacement at a time $t + \Delta t$ is not dependent of the load at that time. The displacement is in fact dependent of the load history of previous time only (present time excluded) in view of the approximations adopted (Eq. (8)) as shown by Eqs. (25) and/or (30).

Besides the efficiency (when compared to classical nodal frequency-domain procedures), the computational simplicity of the non-linear algorithm here presented (see Eq. (30)) and its good accuracy (as shown in the next section) deserve to be highlighted. In fact, the ImFGA method described here is a quite interesting option to analyze dynamic linear or non-linear models.

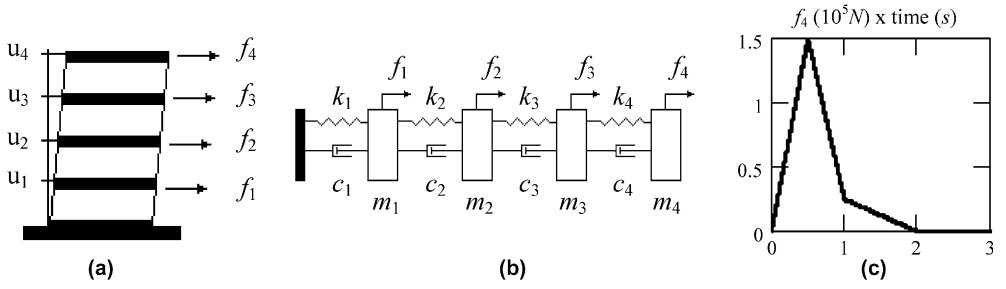

Fig. 2. Shear building: (a) four-store shear building model; (b) equivalent spring-dashpot-mass model; (c) load applied at the fourth floor.

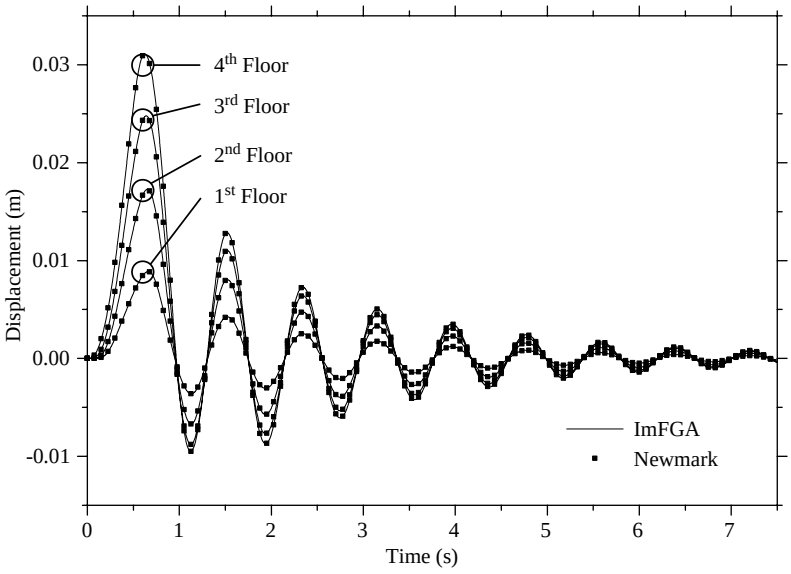

Fig. 3. Displacements obtained for the shear building floors by the ImFGA and the Newmark method.

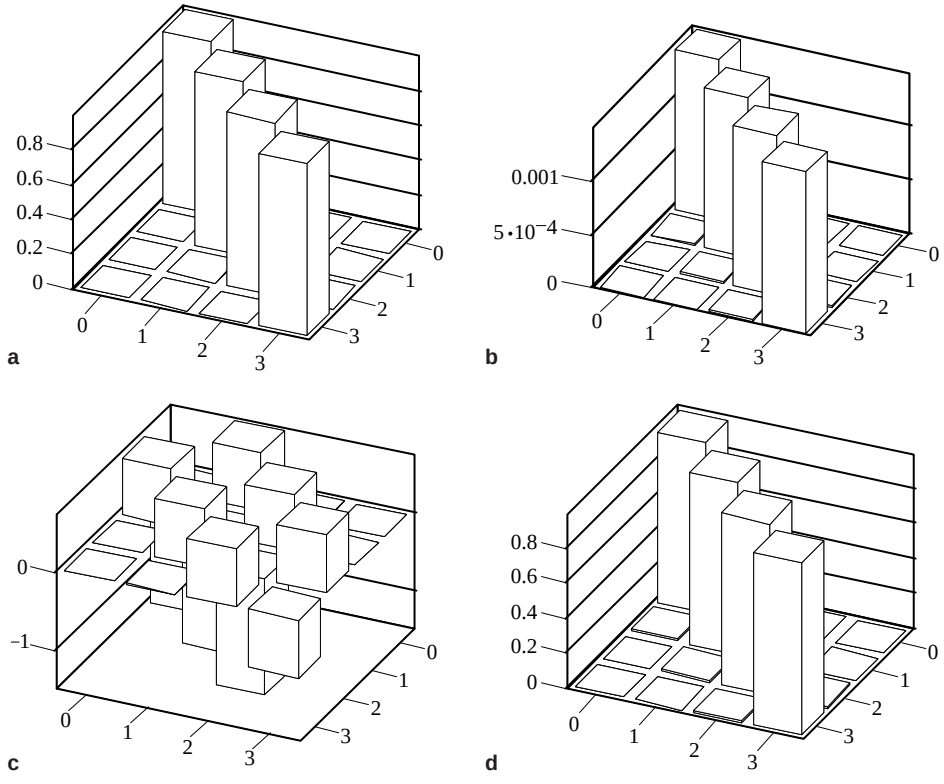

Fig. 4. ImFGA matrices of example 1: (a) $\mathbf{\Phi}_1$; (b) $\mathbf{\Phi}_2$; (c) $\dot{\mathbf{\Phi}}_1$; and (d) $\dot{\mathbf{\Phi}}_2$.

5. Numerical examples

5.1. Preliminary remarks

All the results here presented are compared with those obtained through the classical Newmark method (trapezoidal rule). In the first example a very simple linear model is analyzed; in the second one, an elasto-plastic model is considered.

For all the examples here presented, it was adopted $MT = 1$. In the second example, a Newmark/Newton–Raphson iterative methodology was considered for the time domain comparative analysis. A tolerance of 10^{-3} was then adopted (displacements and force residuals).

The ImFGA matrices ($\mathbf{\Phi}_1, \mathbf{\Phi}_2, \dot{\mathbf{\Phi}}_1$ and $\dot{\mathbf{\Phi}}_2$) are shown graphically in each example. As it can be seen, these matrices present strong diagonal dominance, as it would be expect due to the causality principle. This property can be explored in future research work.

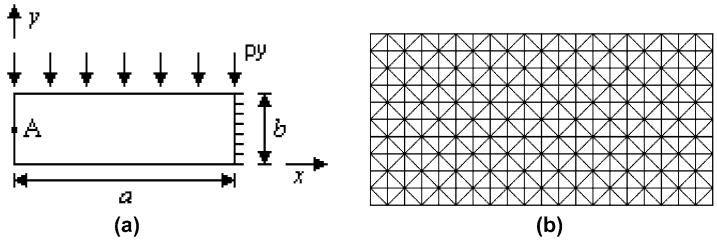

Fig. 5. Clamped beam: (a) geometry and boundary conditions and (b) finite element mesh.

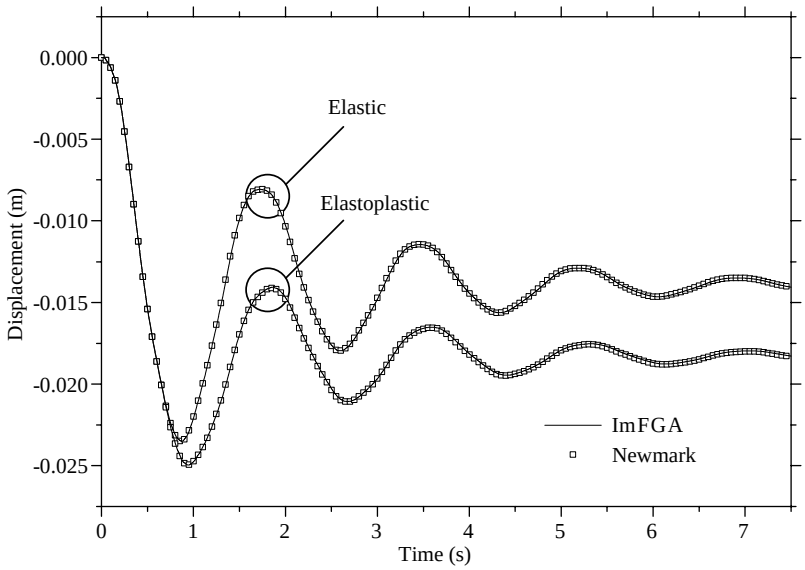

Fig. 6. Vertical displacements time history at point A $(a, b/2)$ for elastic and elasto-plastic analyses by the ImFGA and the Newmark method.

5.2. Example 1

This example considers the simple four-store shear building shown in Fig. 2. The mass and the stiffness values were adopted the same for all floors. They are: mass $= 5.0 \times 10^4$ N s^2/m; stiffness $= 2.5 \times 10^7$ N/m. The damping matrix was considered proportional to the stiffness matrix with a proportionality coefficient equals to 1.5×10^{-2}. The time-step adopted was $\Delta t = 1.5 \times 10^{-3}$ s. A force whose time dependence is shown in Fig. 2(c) was applied at the fourth floor of the model.

Fig. 3 shows the displacements obtained for the shear building floors for the ImFGA and the Newmark methods. A very good agreement can be observed between the two different methods' results. The matrices related to the ImFGA algorithm (Eq. (25)) can be seen graphically in Fig. 4.

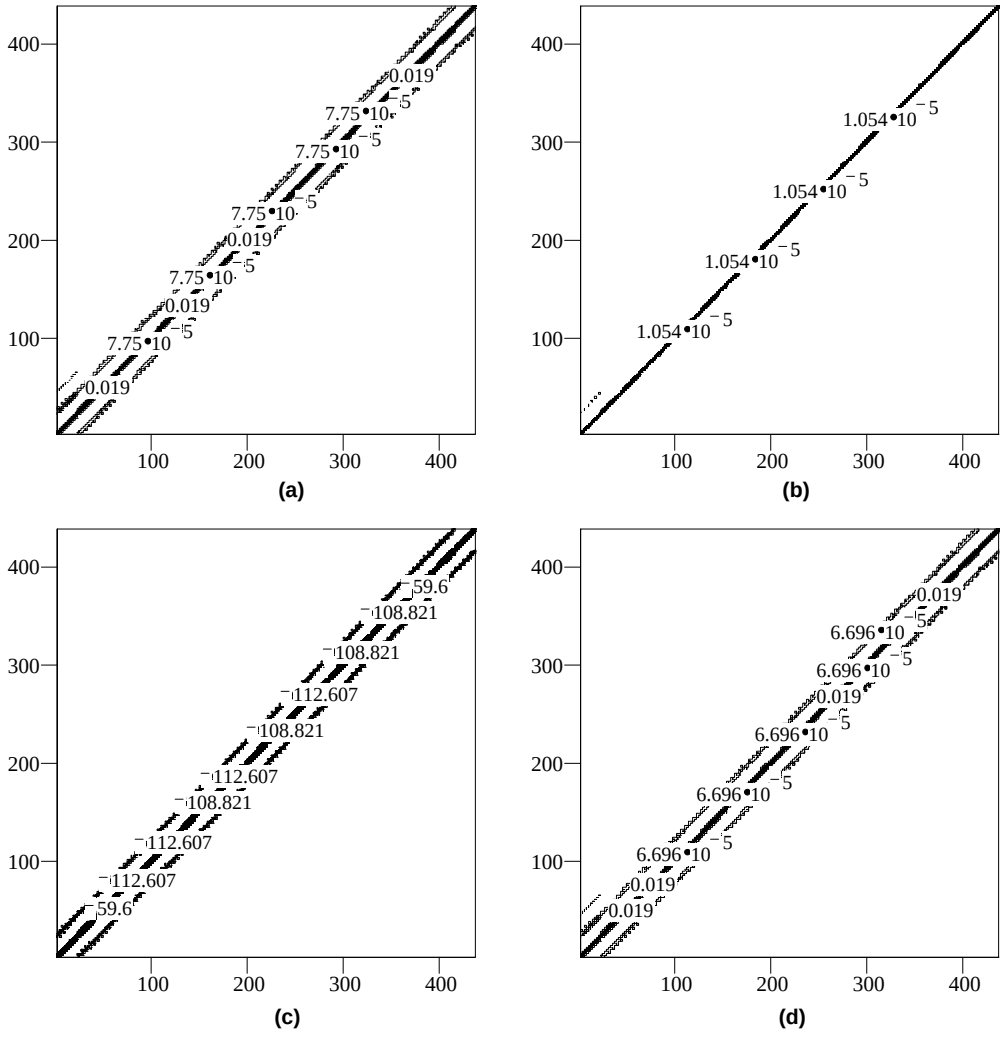

Fig. 7. ImFGA matrices of example 2: (a) $\mathbf{\Phi}_1$; (b) $\mathbf{\Phi}_2$; (c) $\dot{\mathbf{\Phi}}_1$; and (d) $\dot{\mathbf{\Phi}}_2$.

5.3. Example 2

In this example a clamped beam is considered. The geometry, boundary conditions and finite element mesh adopted can be seen in Fig. 5. Four hundred linear triangular isoparametric finite elements were employed. The geometry of the model is defined by $a = 1.0$ m and $b = 0.5$ m.

The clamped beam is submitted to a suddenly applied load, which is kept constant along time. The perfect plastic material is assumed to obey the von Mises yield criterion. The material properties are: Poisson's ratio $= 0.0$; Young modulus $= 100.0$ N/m^2; mass density $= 1.5$ N s^2/m^4; uniaxial yield stress $= 1.0$ N/m^2. A time-step $\Delta t = 10^{-3}$ s was considered in this analysis. The damping matrix was considered proportional to the mass matrix with a proportionality coefficient equals to 1.0 ($\mathbf{C} = \mathbf{M}$).

Fig. 6 shows the vertical displacements obtained at point A (see Fig. 5) considering elastic and elasto-plastic models for the ImFGA and the Newmark method. Once more, a very good agreement can be observed between the different methodology results. The matrices related with the ImFGA algorithm (Eq. (30)) can be seen graphically in Fig. 7.

6. Conclusions

This paper presents a hybrid time-frequency-domain time-stepping FEM procedure to integrate the equations of motion in nodal coordinates. The approach described here, named ImFGA, is based on the mechanical system Green's function, which is implicitly computed in the frequency domain. The pseudo-force method, which was employed here to deal with elasto-plastic material behavior, leads to an iteration free time-stepping algorithm, as the time domain mechanical system Green's function is null at the initial time. Besides being, at each time-step, a low CPU time approach, the accuracy of the ImFGA algorithm is quite good as shown by both the linear and non-linear examples presented in the paper.

References

Aprile, A., Benedetti, A., Trombetti, T., 1994. On non-linear dynamic analysis in the frequency domain. Earthquake Eng. Struct. Dyn. 3, 363–388.

Bathe, K.J., 1996. Finite Element Procedures. Prentice-Hall, Englewood Cliffs, NJ.

Bishop, R.E.D., 1955. The treatment of damping forces in vibration theory. J. Roy. Aeronaut. Soc. 59, 738–742.

Bracewell, R.N., 1986. The Fourier Transform and Its Applications, second ed. McGraw-Hill International Editions, New York.

Clough, R.W., Penzien, J., 1993. Dynamics of Structures, second ed. McGraw-Hill, New York.

Crandall, S.H., 1963. Dynamic response of systems with structural damping. In: Lees, S. (Ed.), Air, Space and Instruments, Draper anniversary volume. McGraw-Hill, Inc., New York, N.Y., pp. 183–193.

Crandall, S.H., 1970. The role of damping in vibration theory. J. Sound Vibr. 11, 3–18.

Crandall, S.H., 1991. The hysteretic damping model in vibration theory. In: Proc. Inst. Mech. Eng., vol. 205, London, UK, pp. 23–28.

Dominguez, J., 1993. Boundary Elements in Dynamics. Computational Mechanics Publications, Southampton and Boston.

Fung, T.C., 1997. A precise time-step integration method by step-response and impulsive-response matrices for dynamic problems. Int. J. Numer. Methods Eng. 40, 4501–4527.

Hughes, T.J.R., 1987. The Finite Element Method. Dover Publications INC, New York.

Jennings, P.C., Bielak, J., 1973. Dynamics of building soil interaction. Bull. Seismol. Soc. Am. 63, 9–48.

Kawamoto, J.D., 1983. Solution of nonlinear dynamic structural systems by a hybrid frequency–time domain approach. In: MIT Research Report R83-5, Department of Civil Engineering.

Liu, S.C., Fagel, L.W., 1971. Earthquake interaction by fast Fourier transform. J. Eng. Mech. Div. ASCE 97, 1223–1237.

Makris, N., 1997. Causal hysteretic element. J. Eng. Mech., ASCE 123, 1209–1214.

Makris, N., Zhang, J., 2000. Time-domain viscoelastic analysis of earth structures. Earthquake Eng. Struct. Dyn. 29, 745–768.

Mansur, W.J., 1983. A time-stepping technique to solve wave propagation problems using the boundary element method. Ph.D. Thesis, University of Southampton, England.

Mansur, W.J., Ferreira, W.G., Claret, A.M., Venancio-Filho, F., Carrer, J.A.M., 2000. Time-segmented frequency-domain analysis for non-linear multi-degree-of-freedom structural systems. J. Sound Vibr. 237, 458–475.

Mansur, W.J., Soares Jr., D., Ferro, M.A.C., 2004. Initial conditions in frequency-domain analysis: the FEM applied to the scalar wave equation. J. Sound Vibr. 270, 767–780.

Matthees, W., 1982. A strategy for the solution of soil dynamic problems involving plasticity by transform. Int. J. Numer. Methods Eng. 18, 1601–1611.

Myklestad, N.O., 1952. The concept of complex damping. J. Appl. Mech., ASME 19, 284–286.

Newmark, S., 1957. Concept of complex stiffness applied to problems of oscillations with viscous and hysteretic damping. Aeronaut. Res. Council Rep. 3269, 1–34.

Newland, D.E., 1993. An Introduction to Random Vibration, Spectral & Wavelet Analysis, third ed. Longman Scientific & Technical, New York.

Oppenheim, A.V., Schafer, R.W., 1989. Discrete Time Signal Processing. Prentice-Hall, Englewood Cliffs, NJ.

Paz, M., 1997. Structural Dynamics—Theory and Computation, fourth ed. Chapman and Hall, New York.

Proakis, J.G., Manolakis, D.G., 1996. Digital Signal Processing-Principles. Algorithms and Applications, third ed. Prentice-Hall, Englewood Cliffs, NJ.

Soares Jr., D., Mansur, W.J., 2003. An efficient time/frequency domain algorithm for modal analysis of non-linear models discretized by the FEM. Comput. Methods Appl. Mech. Eng. 192, 3731–3745.

Soares Jr., D., Mansur, W.J., 2005. A Time Domain FEM approach based on implicit Green's functions for non-linear dynamic analysis. Int. J. Numer. Methods Eng. 62, 664–681.

Takewaki, I., Nakamura, M., 2000. Stiffness-damping simultaneous identification using limited earthquake records. Earthquake Eng. Struct. Dyn. 29, 1219–1238.

Theodorsen, T., Garrick, I.E., 1940. Mechanism of flutter, a theoretical and experimental investigation of the flutter problem. Report No. 685, Natl. Advisory Comm. for Aeronautics, Washington, DC.

Veletsos, A., Ventura, C., 1984. Efficient analysis of dynamic response of linear systems. Earthquake Eng. Struct. Dyn. 12, 521–536.

Veletsos, A., Ventura, C., 1985. Dynamic analysis of structures by the DFT method. J. Struct. Eng., ASCE 111, 2625–2642.

Venâncio-Filho, F., Claret, A.M., 1991. An implicit Fourier transform method for nonlinear dynamic analysis with frequency dependent damping. Damping Conference, San Diego, CA.

Venancio-Filho, F., Claret, A.M., 1992. Matrix formulation of the dynamic analysis of SDOF in frequency domain. Comput. Struct. 42, 853–855.

Wu, W.H., Smith, H.A., 1995. Efficient modal analysis for structures with soil–structure interaction. Earthquake Eng. Struct. Dyn. 24, 283–299.

Wolf, J.P., 1985. Dynamic Soil–Structure Interaction. Prentice-Hall, Englewood Cliffs, NJ.

Zienkiewicz, O.C., Taylor, R.L., 1989The Finite Element Method, vol. I and II. McGrawHill, London.